Proc. Natl. Acad. Sci. USA
Vol. 76, No. 8, pp. 4071–4074, August 1979
Immunology

Crystal structure of galactan-binding mouse immunoglobulin J539 Fab at 4.5-Å resolution

(x-ray diffraction/pattern recognition/antibody structure)

MANUEL A. NAVIA*, DAVID M. SEGAL*†, EDUARDO A. PADLAN*‡, DAVID R. DAVIES*, NARAYANA RAO§, STUART RUDIKOFF§, AND MICHAEL POTTER§

*Laboratory of Molecular Biology, National Institute of Arthritis, Metabolism and Digestive Diseases; and §Laboratory of Cell Biology, National Cancer Institute, National Institutes of Health, Bethesda, Maryland 20205

Contributed by David R. Davies, May 11, 1979

ABSTRACT **An electron-density map of the mouse galactan-binding immunoglobulin J539 (IgA2,κ) Fab has been calculated to a resolution of 4.5 Å by the method of heavy atom isomorphous replacement with four derivatives. The map has been interpreted with the aid of a computer program which systematically searched for the best fit between the electron-density map and the known coordinates of individual immunoglobulin domains. The quaternary structure of J539 Fab at this resolution appears similar to that of another mouse immunoglobulin, IgA2,κ Fab, McPC603. The model coordinates for J539 Fab should allow us to proceed directly to a high-resolution structure determination without further heavy atom isomorphous replacement.**

The crystal structures of three immunoglobulin Fabs have been reported (1–3). One of these, the mouse myeloma protein McPC603, belongs to a class of immunoglobulins that bind specifically to phosphocholine. In this paper, we present the results of a structural analysis at 4.5-Å resolution of a second mouse Fab, the galactan-binding immunoglobulin J539. A molecular model has been constructed with the aid of a computer search procedure used previously in the interpretation of the electron-density map of an intact immunoglobulin (4). The model allows us to describe the quaternary structural interactions between the constituent domains and domain pairs of the J539 Fab and reveals a general similarity to McPC603.

MATERIALS AND METHODS

The immunoglobulin J539 [a mouse IgA2,κ; anti-(1→6)-β-D-galactan] was isolated and purified as described (5), and pepsin fragments were obtained by using a published procedure (6).

Crystals of J539 Fab were grown at room temperature from 35% saturated solutions of ammonium sulfate containing 0.07 M imidazole and 0.03 M zinc sulfate at pH 6.8. The crystals exhibit the symmetry of space group $P2_12_12_1$ with unit cell dimensions: a = 54.1 Å, b = 74.2, Å, and c = 130.8 Å. They diffract to a resolution of at least 2.5 Å. Prior to further work, the crystals were transferred into stabilizing solution (45% saturated ammonium sulfate/0.07 M imidazole/0.03 M zinc sulfate, pH 6.8). On rare occasions, a second crystal form was observed in the space group $P2_12_12_1$ with unit cell dimensions: a = 55.7 Å, b = 74.1 Å, and c = 125.7 Å. Cocrystallization in the presence of the haptens (1→6)-β-D-galactodiose (Gal_2) and (1→6)-β-D-galactotetraose (Gal_4), both kindly provided by C.P.J. Glaudemans, yielded a needle-like crystal form which remains uncharacterized.

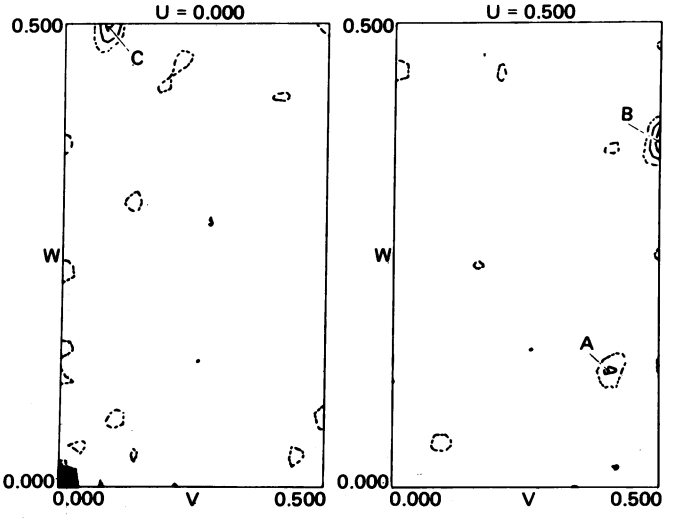

FIG. 1. Sections through the difference Patterson map for the $K_2Pt(CNS)_6$ derivative, showing the Harker peaks (A, B, and C). Contours are at 1/40ths of origin peak; zero and negative contours are omitted.

Useful heavy atom derivatives were obtained by soaking J539 Fab crystals in stabilizing solutions with 0.25 mM $K_2Pt(CNS)_6$ for 2 weeks, 1 mM K_2PtCl_4 for 1 week, 0.3 mM K_2HgI_4 for 2 weeks, and 50 mM KI/1 mM chloramine-T (Eastman Kodak) for 1 week. The iodine-derivatized crystals were washed with fresh stabilizing solution after the soaking period. Unique sets of three-dimensional reflection data to 4.5-Å spacings were collected from native and derivative crystals with a Picker FACS-1 diffractometer operated in the ω-scan mode and using Cu Kα radiation. The various data sets were placed on the same relative scale, and pseudo temperature factors were applied to correct for differences in intensity fall-off. The $K_2Pt(CNS)_6$ derivative was analyzed first, and difference Patterson maps, readily interpretable, revealed one site of substitution (Fig. 1). After preliminary refinement with projection data only, the coordinates and occupancy of the $K_2Pt(CNS)_6$ site were used to determine the signs of the centric native protein reflections. These signs were used to examine the K_2PtCl_4 and K_2HgI_4 derivatives by difference Fourier analysis. The variables for these three heavy atom derivatives were then subjected to alternating cycles of least squares refinement and phase determination with the three-dimensional data. The resulting phases

The publication costs of this article were defrayed in part by page charge payment. This article must therefore be hereby marked "*advertisement*" in accordance with 18 U. S. C. §1734 solely to indicate this fact.

† Present address: Immunology Branch, National Cancer Institute.
‡ Present address: Biophysics Department, Johns Hopkins University, Baltimore, MD.

Table 1. Heavy atom variables after refinement

Derivative	Site	Rel. occupancy*	Fractional coordinates X	Y	Z	Isotropic temperature factor, Å^2	R_c†	R_k‡	E§
$K_2Pt(CNS)_6$	1	1.00	0.2320	0.0437	0.0624	22.1	0.507	0.068	0.95
K_2PtCl_4	1	0.51	0.2304	0.0477	0.0627	18.8	0.590	0.068	0.89
	2	0.51	0.6143	0.0333	0.3444	25.1			
K_2HgI_4	1	0.62	0.6346	0.0550	0.3477	25.6	0.606	0.070	0.92
Iodine	1	0.62	0.5425	0.4514	0.5867	25.6	0.587	0.116	1.62
	2	0.96	0.6349	0.8920	0.4008	13.0			
	3	0.32	0.2927	0.1535	0.3469	22.2			

* The site occupancies are on an arbitrary scale with the $K_2Pt(CNS)_6$ site assigned an occupancy of 1.00.
† $R_c = \Sigma||F_{PH} - F_P| - F_H|/\Sigma|F_{PH} - F_P|$, in which the sums are over centric reflections only.
‡ $R_k = \Sigma||F_{PH}| - |F_P + F_H||/\Sigma|F_{PH}|$.
§ E is the root mean square lack of closure error. The average protein structure amplitude is 10.3.

were subsequently used to analyze the iodine derivative. The refined variables of the four heavy atom derivatives are listed in Table 1. The mean figure-of-merit for the 1895 phased reflections is 0.82. "Best" (7) Fourier maps were computed by using these phases.

Two methods were used to interpret this map.

(*i*) Visual examination of the map, making use of the known structure of McPC603. In addition, because $K_2Pt(CNS)_6$ bound also to McPC603 where it was attached to the constant region of the molecule (8) and because the constant regions of McPC603 and J539 Fab are most probably identical, it was assumed that $Pt(CNS)_6^{2-}$ bound to the same site in both molecules, thus providing a known location in J539 from which to start the interpretation.

(*ii*) The overall three-dimensional structures of the domains of McPC603 were assumed to be similar to those of J539. A computer program was accordingly used to rotate and translate exhaustively the known coordinates of the domains of McPC603 Fab (9) into the electron-density map of J539; after each such transformation, they were compared with the density. The criterion of fit was the number of overlaps of transformed coordinates on the electron density. This program was originally used in the interpretation of the electron-density map of the intact immunoglobulin "Dob" (4) and will be described in detail elsewhere. The translations of the domains were conducted along the three orthogonal axes with increments of 2 Å at 6.0-Å resolution and of 1.5 Å at 4.5-Å resolution. The rotations were computed by varying the three Eulerian angles with increments of 30° at 6.0-Å resolution and of 15° at 4.5-Å resolution (these increments were decreased as the final fit solution was approached). To further limit the scope of the search, the coordinates of McPC603 heavy chain residue 148, which in McPC 603 was near the $K_2Pt(CNS)_6$ binding site, was tethered to within 20 Å of the coordinates of the platinum binding site in the J539 electron-density map, again on the assumption that both molecules have the same Pt binding site.

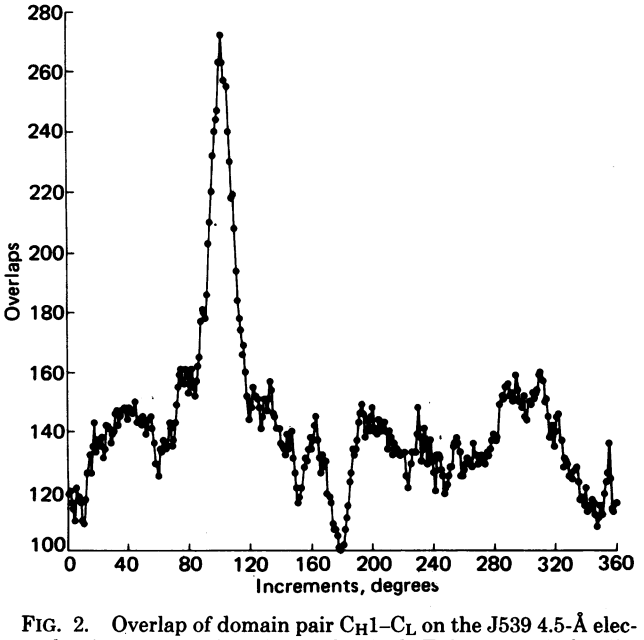

FIG. 2. Overlap of domain pair C_H1–C_L on the J539 4.5-Å electron-density map as a function of the single Eulerian angle $\theta 1$. The angle was systematically varied in 1° intervals over its full range with all other rotation and translation variables fixed at their maximal overlap values.

For the initial search at 6-Å resolution, the constant region domain pair (C_H1–C_L) of McPC603 Fab was used as a unit. Afterwards, the variable region domain pair (V_H–V_L) was used as a unit, with the hypervariable residues (10) for the light chain, 26–34, 50–55, and 92–96, and for the heavy chain, 31–35, 51–59, and 97–100, omitted because they could be expected to differ between McPC603 and J539. At this stage of the search, only α-carbon coordinates were used in order to minimize computer time and the amount of memory used. All searches were conducted on a PDP 11/70 computer which has an addressing limit of 32,000 words.

The 6-Å resolution results were refined by searches of the 4.5-Å resolution J539 map. This time, however, the individual McPC603 domains (C_H1, C_L, V_H, V_L) were fitted separately. An idealized (11) polyalanine structure, generated from the McPC603 backbone coordinates and again excluding hypervariable residues, was used in the search. Typical results for the two searches are presented in Table 2 and Fig. 2. An indication of the precision of the fit obtained by this procedure can be

Table 2. Comparison of search results using the C_H1–C_L domain pair at two resolutions

Resolution, Å	No. of atoms used in search	Overlaps,* no. Maximum	Mean	Peak height above mean, SD
6	208	93	46	3.9
4.5	1020	503	305	4.8

The Euler angle $\theta 1$ was systematically varied about the final C_H1–C_L domain-pair solution; all other rotation/translation variables were kept fixed.
* "Overlaps" refer to the number of coordinates found to superimpose on electron density above a specified level (see text).

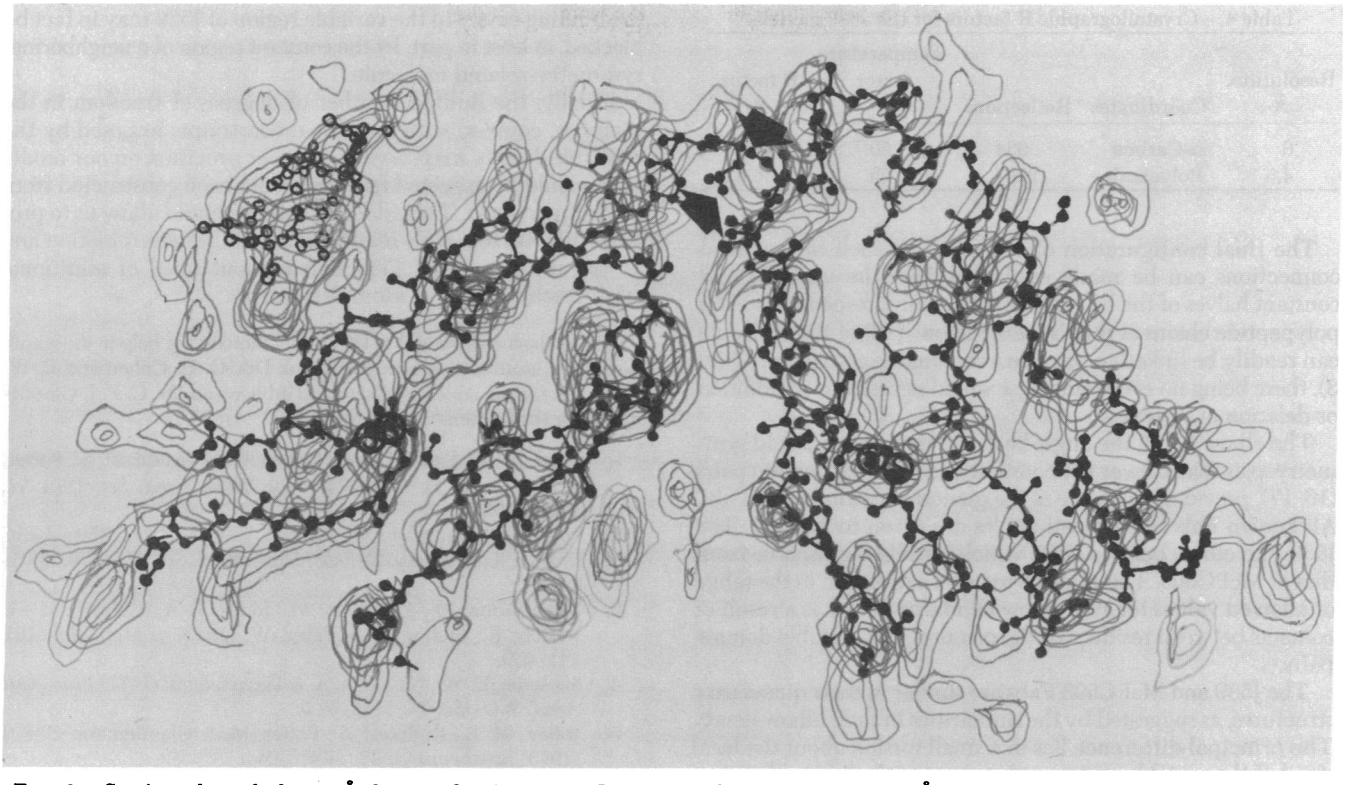

FIG. 3. Sections through the 4.5-Å electron-density map of J539 perpendicular to the *Y* (74.2 Å) axis, with model polyalanine coordinates superimposed. The sections shown are from y = 0.06 to y = 0.16. Solid and open circles, heavy and light chains, respectively; arrows, ends of the independently fitted V_H and C_H1 domains that have to be joined at the switch region.

obtained from the Euler angle solutions presented in Table 3. Another estimate of the precision of fit might be obtained from the width of the curve in Fig. 2. A quantitative estimate is difficult, however, because the error cannot be demonstrated to have a normal distribution but seems to depend rather on the form and pseudosymmetry of the fitted molecule. The solution peak for the 6-Å search was broader than that for the 4.5-Å search, thus justifying the use of a coarser and more economical sampling scheme at the lower resolution.

RESULTS AND DISCUSSION

Examination of more than 50 heavy atom compounds yielded only the four usable derivatives of Table 1. For reasons that were not apparent, these derivatives were of significantly poorer quality than those used for the comparable McPC603 analysis (8), and their use led to an electron-density map in which the contrast between protein and solvent regions was low, so that the molecular boundary was not immediately apparent. An attempt to interpret this map visually based on the positions of the heavy atom derivatives, particularly $K_2Pt(CNS)_6$, and the known structure of McPC603 Fab resulted in a tentative delineation of the molecular boundary. However, interpretation of the electron-density map in specific molecular terms necessitated a more quantitative approach.

Table 3. "Best-fit" Euler angles at two resolutions and for the constant domains taken separately and in pairs

Resolution,	C_H1–C_L			C_H1			C_L		
Å	$\theta 1$	$\theta 2$	$\theta 3$	$\theta 1$	$\theta 2$	$\theta 3$	$\theta 1$	$\theta 2$	$\theta 3$
6	105	336	99						
4.5	99	332	113	100	334	111	106	328	110

The electron-density maps used in the search procedure were sampled at one-third the resolution indicated.

The search procedure described above was carried out independently of the visual interpretation and ultimately led to a best fit solution (Figs. 3 and 4). We have calculated structure factors and crystallographic R factors for the molecular models resulting from both the high- and low-resolution searches (Table 4). These numbers compare favorably with the R factors of other structures at similar stages of their solution (12–15).

In the search procedure at 4.5-Å resolution, the individual domains were fitted separately and their final positions in the model correspond to the highest peak of overlap. Nothing in this search procedure constrains the separate domains to a well-behaved and consistent solution. It is therefore reassuring that the domains do not interpenetrate. Also, the packing of the molecules in the unit cell, taking into account the symmetry elements of the space group $P2_12_12_1$, provides an arrangement in which neighboring molecules do not share density but nevertheless appear to make sufficient intermolecular contacts to sustain a crystal lattice.

FIG. 4. Stereo view of the Cα skeleton of the J539 Fab structure. Open circles, McPC603 hypervariable residues that were excluded from the search.

Table 4. Crystallographic R factors for the J539 models

Resolution, Å	Coordinates	Reflections	Temperature factor, Å²	R factor, %
6	α-Carbon	934	50	44.7
4.5	Polyalanine	2167	25	46.5

The final configuration of the model is such that natural connections can be made easily between the variable and constant halves of the heavy and light chains, respectively. The polypeptide chains at this "switch region" (16) of the molecule can readily be linked to provide a reasonable connection (Fig. 3), there being no constraints that would necessitate an addition or deletion of residues.

The elbow bend, the angle between the pseudo 2-fold symmetry axes that skewer the constant and variable domain pairs (16, 17), provides a measure of the quaternary structure of Fabs. All known Fab elbow bend angles are given in Table 5. The J539 Fab elbow bend is 136°, which is indistinguishable from that of McPC603. This appears to be an extremum in the range of allowed values for Fab elbow bends, probably as a result of contacts between residues of the constant and variable domain pairs.

The J539 and McPC603 Fabs are similar in their quaternary structures, as suggested by the similarities in their elbow bends. The principal difference lies in a small torsion about the local dyad of the variable region with respect to the constant region. Note that the resolution of the electron-density map is too low to provide any information about the conformations of the various hypervariable regions of J539; these should be revealed with the future high-resolution refinement of the structure.

The model can provide a plausible explanation for the observation that soaking of the haptens Gal_2 and Gal_4 into J539 crystals did not yield significant intensity changes indicative of binding. Examination of the molecular packing shows that the binding cavity in the variable region of J539 may in fact be blocked, at least in part, by the constant region of a neighboring, symmetry-related molecule.

Table 5. Published Fab elbow bend angles

Protein (ref.)	Angle, degrees
Newm (2)	131*
McPC603 (1)	134
J539 (this work)	136
Dob IgG (4)	147
Kol Fab (3)	166
Kol IgG (17)	174

* This elbow bend angle was computed from coordinates in AMSOM (9).

Finally, the limited number of degrees of freedom in the searches, coupled with the global constraints imposed by the electron-density map, confer a higher precision on our model than would be expected had the model been constructed from the map *de novo*. This added precision should allow us to proceed directly to a high-resolution structure determination and to the refinement of J539 Fab without need of additional high-resolution heavy atom derivatives.

The authors are grateful to Dr. Daniel Mercola for help in the search for heavy atom derivatives. We thank Drs. G. H. Cohen and E. W. Silverton for valuable discussion and advice and Dr. C. P. J. Glaudemans for the haptens used in this study.

1. Segal, D. M., Padlan, E. A., Cohen, G. H., Rudikoff, S., Potter, M. & Davies, D. R. (1974) *Proc. Natl. Acad. Sci. USA* **71**, 4298–4302.
2. Poljak, R. J., Amzel, L. M., Avey, H. P., Chen, B. L., Phizackerly, R. P. & Saul, F. (1973) *Proc. Natl. Acad. Sci. USA* **70**, 3305–3310.
3. Matsushima, M., Marquart, M., Jones, T. A., Colman, P. M., Bartels, K., Huber, R. & Palm, W. (1978) *J. Mol. Biol.* **121**, 441–459.
4. Silverton, E. W., Navia, M. A. & Davies, D. R. (1977) *Proc. Natl. Acad. Sci. USA* **74**, 5140–5144.
5. Jolley, M. E., Rudikoff, S., Potter, M. & Glaudemans, C. P. J. (1973) *Biochemistry* **12**, 3039–3044.
6. Rudikoff, S., Potter, M., Segal, D. M., Padlan, E. A. & Davies, D. R. (1972) *Proc. Natl. Acad. Sci. USA* **69**, 3689–3692.
7. Blow, D. M. & Crick, F. H. C. (1959) *Acta Crystallogr.* **12**, 794–802.
8. Padlan, E. A., Segal, D. M., Spande, T. F., Davies, D. R., Rudikoff, S. & Potter, M. (1973) *Nature (London) New Biol.* **145**, 165–167.
9. Feldmann, R. J., ed. (1976) *AMSOM-Atlas of Macromolecular Structure on Microfiche* (Tracor Jitco, Inc., Rockville, MD).
10. Kabat, E. A., Wu, T. T. & Bilofsky, H. (1976) in *Variable Regions of Immunoglobulin Chains* (Medical Computer Systems, Bolt, Beranek & Newman, Cambridge, MA).
11. Diamond, R. (1966) *Acta Crystallogr.* **21**, 253–266.
12. Schmid, M. F., Herriott, J. R. & Lattman, E. A. (1974) *J. Mol. Biol.* **84**, 97–101.
13. Wishner, B. C., Ward, K. B., Lattman, E. A. & Love, W. E. (1975) *J. Mol. Biol.* **98**, 179–194.
14. Ward, K. B., Hendrickson, W. A. & Klippenstein, G. L. (1975) *Nature (London)* **257**, 818–821.
15. Sarma, R. & Bott, R. (1977) *J. Mol. Biol.* **113**, 555–565.
16. Davies, D. R., Padlan, E. A. & Segal, D. M. (1975) in *Contemporary Topics in Molecular Immunology*, eds. Inman, F. P. & Mandy, W. J. (Plenum, New York), Vol. 4, pp. 127–155.
17. Colman, P. M., Deisenhofer, J., Huber, R. & Palm, W. (1976) *J. Mol. Biol.* **100**, 257–282.